Targeting Estrogen Receptor-Positive Breast Microtumors with Endoxifen-Conjugated, Hypoxia-Sensitive Polymersomes

Babak Mamnoon, Li Feng, Jamie Froberg, Yongki Choi, Venkatachalem Sathish, Oleh Taratula, Olena Taratula, and Sanku Mallik*
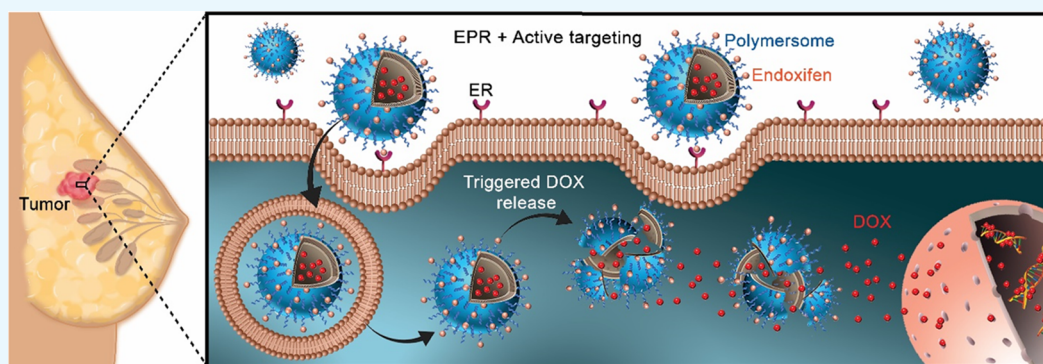
Read Online

ACCESS | Metrics & More | Article Recommendations | Supporting Information

ABSTRACT: Endoxifen is the primary active metabolite of tamoxifen, a nonsteroidal-selective estrogen receptor modulator (SERM) and widely used medication to treat estrogen receptor-positive (ER+) breast cancer. In this study, endoxifen was conjugated to the surface of polymeric nanoparticles (polymersomes) for targeted delivery of doxorubicin (DOX) to estrogen receptor-positive breast cancer cells (MCF7). Rapid cell growth and insufficient blood supply result in low oxygen concentration (hypoxia) within the solid breast tumors. The polymersomes developed here are prepared from amphiphilic copolymers of polylactic acid (PLA) and poly(ethylene glycol) (PEG) containing diazobenzene as the hypoxia-responsive linker. We prepared two nanoparticle formulations: DOX-encapsulated hypoxia-responsive polymersomes (DOX-HRPs) and endoxifen-conjugated, DOX-encapsulated hypoxia-responsive polymersomes (END-DOX-HRPs). Cellular internalization studies demonstrated eight times higher cytosolic and nuclear localization after incubating breast cancer cells with END-DOX-HRPs (targeted polymersomes) in contrast to DOX-HRPs (nontargeted polymersomes). Cytotoxicity studies on monolayer cell cultures exhibited that END-DOX-HRPs were three times more toxic to ER+ MCF7 cells than DOX-HRPs and free DOX in hypoxia. The cell viability studies on three-dimensional hypoxic cultures also demonstrated twice as much toxicity when the spheroids were treated with targeted polymersomes instead of nontargeted counterparts. This is the first report of surface-decorated polymeric nanoparticles with endoxifen ligands for targeted drug delivery to ER+ breast cancer microtumors. The newly designed endoxifen-conjugated, hypoxia-responsive polymersomes might have translational potential for ER+ breast cancer treatment.

1. INTRODUCTION

Breast cancer (BC) is characterized by uncontrolled cell proliferation, angiogenesis, and metastasis to other organs.[1] Surgery and radiation therapy are effective treatment options for the localized disease.[2] Hormone therapy and chemotherapy are the most common regimen for invasive BC.[3] Unfortunately, chemotherapeutic agents show various side effects that limit their administration in cancer therapy.[4–7] In addition, low solubility, high therapeutic dosage, reduced systemic blood circulation, and increased cytotoxicity are common drawbacks of anticancer drugs.[8,9] Uncontrolled cell proliferation and limited blood flow generate low oxygen concentration (hypoxia) in solid tumor tissues of various cancers, including

BC[10–14] leading to invasiveness, metastasis, and drug resistance.[15,16]

Nanomedicine and nanotechnology are emerging fields in drug delivery, diagnosis, and the development of nanoscale materials for cancer therapy.[17–20] Nanocarrier-based drug delivery systems can address the shortcomings of traditional chemotherapy by improving circulation half-life, tumor

penetration, and cellular internalization.[21,22] Among various nanoparticles, polymersomes show considerable promise to deliver drugs into cancerous tissues.[23] They are self-assembled bilayer vesicles prepared from amphiphilic copolymers with hydrophilic and hydrophobic blocks.[24−26] Vesicle formation is favored when the molecular weight ratio of the hydrophilic block to the whole polymer is between 20 to 40%.[10,24,27] Polymersomes carry hydrophilic drugs within the aqueous core and hydrophobic drugs inside the bilayer simultaneously.[12,28] Poly(ethylene glycol) (PEG) is commonly used as a hydrophilic block due to its biocompatibility, reduction in plasma protein adsorption, and the resultant prolonged circulation time of the polymersomes.[29]

Because of the higher molecular weights of the polymers compared to lipids, polymersomes are more robust and stable than liposomes.[28] However, enhanced stability requires a stimulus for releasing the encapsulated drugs.[29,30] The stimuli-responsive polymersomes are stable in systemic circulation and disintegrate within the disease sites by responding to physical, chemical, or biological stimuli.[31−34] Hypoxia-responsive polymersomes release therapeutic agents under low oxygen partial pressure within solid tumors.[10−12] In addition, modifying polymersomes' surface with ligands for selective binding to an overexpressed receptor on cancer cells facilitates tumor penetration and cellular internalization, hence, reducing the off-target side effects of chemotherapeutic agents.[35−39]

Estrogen receptors (ERs) are overexpressed in about 80% of BC cases (ER+ BC).[40] ERs are divided into ERα and ERβ subclasses. A class of ERα (G-protein-coupled receptors) are expressed on the membrane of BC cells.[41] Tamoxifen (TAM) is a pioneering medicine for the ER+ BC treatment that belongs to selective estrogen receptor modulators (SERM).[42] TAM competes with estrogen for binding to ERs and reduces breast tumor growth.[43] TAM can be incorporated as a ligand into nanoparticles' surfaces for targeting overexpressed ERs on BC cells' surfaces.[44] However, TAM is a prodrug that converts to active metabolites, such as 4-hydroxy TAM or endoxifen (END).[43] END is the most active metabolite of TAM. It binds to the ER about 100 times more strongly and about 30 times more potent in reducing the growth and proliferation of ER+ breast cancer cells compared to TAM.[45,46] Accordingly, utilizing END to target ER+ breast cancer cells appears more valuable in solid ER+ breast tumors.

Herein, we conjugated END to an amphiphilic block copolymer of poly(ethylene glycol) (PEG) and polylactic acid (PLA). We prepared polymersomes from the END-conjugated and a hypoxia-responsive copolymer, encapsulating the anticancer drug doxorubicin (DOX) inside. Due to the END ligands, the polymersomes selectively bind to overexpressed ERs on ER+ BC cells' surface, translocate into the cells, disintegrate, and release their chemotherapeutic payload selectively within hypoxic BC cells. According to the previously reported studies, endoxifen was either encapsulated within nanoparticles,[47] or conjugated with other drugs for interacting ER+ breast cancers[48,49] but not as a ligand for selective nanoparticulate drug delivery. To our knowledge, this is the first report of employing END as a high-affinity ligand to target ER+ breast cancer cells by polymersomes. The advantage of this study is to employ endoxifen (100 times more potent compared to tamoxifen) as a surface-conjugated ligand for the selective estrogen receptor interaction. Compared to the previous reports from our group regarding the incorporation of estradiol on the surface of polymeric nanoparticles,[12] the surface conjugation of endoxifen as a ligand makes these new nanoparticles more potent for selective binding to the breast cancer cellular estrogen receptors. Thus, we anticipate that these targeted nanoparticles have a potential for targeted chemotherapeutic drug delivery to ER+ hypoxic tumors. Future studies can be performed to evaluate the efficiency of these newly synthesized targeted nanoparticles in vivo.

2. MATERIALS AND METHODS

2.1. Materials and Reagents. Endoxifen hydrochloride was purchased from Selleckchem. Doxorubicin hydrochloride was purchased from Advanced Chemblocks. Avanti Polar was the provider of the lissamine rhodamine (LR) dye. The chemicals for synthesizing the copolymers were purchased from Millipore Sigma. The medium and antibiotics for the cell culture were purchased from VWR International. A humidified incubator (Thermo Scientific) containing 5% CO_2 and 21% O_2 at 37 °C was used for normoxic conditions. For all experiments, a hypoxia chamber containing 5% CO_2 and 2% O_2 was used.

2.2. Synthesis and Characterization of Copolymers. The polylactate−diazobenzene−poly(ethylene glycol) (PLA_{8500}−Azo−PEG_{2000}) and polylactate−poly(ethylene glycol) azide (PLA_{16000}−PEG_{2000}−N_3) polymers were synthesized and characterized according to the previously reported protocol (Supporting Information, Figures S1−S5).[12] For the synthesis of endoxifen-hexynol, 5-hexyn-1-ol (11 μL, 100 μmol) and triethylamine (0.1 mL) were dissolved in 5 mL of anhydrous dichloromethane. Then, N-(3-dimethylaminopropyl)-N′-ethylcarbodiimide hydrochloride EDC·HCl (27 mg, 100 μmole), N-hydroxysuccinimide (NHS) (11.5 mg, 100 μmole), and dimethylaminopyridine (DMAP) (3 mg, 5% mol) were added, and the mixture was stirred at 25 °C for 1 h under a nitrogen atmosphere. Endoxifen HCl (41 mg, 100 μmole) was added to the reaction mixture and stirred overnight, followed by washing 3 times with water and drying under vacuum to get a solid compound (0.62 g, yield: 40%). ^{1}H-NMR (400 MHz, chloroform-d): 7.13−6.51 ((CH2=CH2), d, 13 H), 4.11 ((CH2-CH_2-N), t, 2 H), 3.99 ((CH_2-O-C= O), t, 2 H), 3.70 ((CH2-CH_2-N), t, 2 H), 3.59 ((CH_3-N), s, 3 H), 3.01 ((CH≡C-), s, 1 H), 2.51 ((CH≡C-CH_2), t, 2 H), 2.24 ((CH_3-CH_2), q, 2 H), 1.65 ((CH_2-CH_2- CH_2), m, 2 H), 1.28 ((CH_2-CH_2- CH_2), m, 2 H), 0.85 ((CH_3-CH_2), t, 3 H). MH+ calcd for $C_{32}H_{35}NO_4$: 498.2646. Found: 498.2644.

Endoxifen-hexynol (7 mg, 10 μmol) and azide polymer (100 mg, 5 μmol) were dissolved in 5 mL of THF. According to a protocol developed in our laboratory, the cycloaddition reaction between endoxifen-hexynol and the azide polymer PLA_{16000}−PEG_{2000}−N_3 was performed with a 97% degree of conjugation.[12] The final product was dried under vacuum (7 mg, yield: 57%) and characterized by ^{1}H-NMR and gel permeation chromatography (GPC, TSKgel Super H3000) using THF as the solvent. ^{1}H-NMR (400 MHz, chloroform-d): 7.00 (C=CH-CH=C, s, 1 H), 5.19 ((-CH-C=O), q, 1 H), 3.67 ((CH2-C=O), d, 2 H), 2.29 ((CH3-NH), d, 3 H), 1.58 ((CH3-CH-C=O), d, 3 H), 0.89 ((CH3-C-), s, 6 H). GPC: M_w = 12 098, M_n = 9368; and PDI = 1.29.

2.3. Polymersome Preparation. Polymers were dissolved in acetone (10 mg/mL), and lissamine rhodamine lipid dye (LR) was dissolved in chloroform (0.01 mg/mL). Plain (HEPES buffer-encapsulated) and nontargeted polymersomes were prepared by adding a 95:5 molar ratio azobenzene polymer to LR. Targeted polymersomes were prepared by

Scheme 1. Cycloaddition Reaction between PLA$_{16000}$–PEG$_{2000}$–N$_3$ Polymer and Alkyne-Endoxifen to Prepare the PLA$_{16000}$–PEG$_{2000}$–Endoxifen Polymer
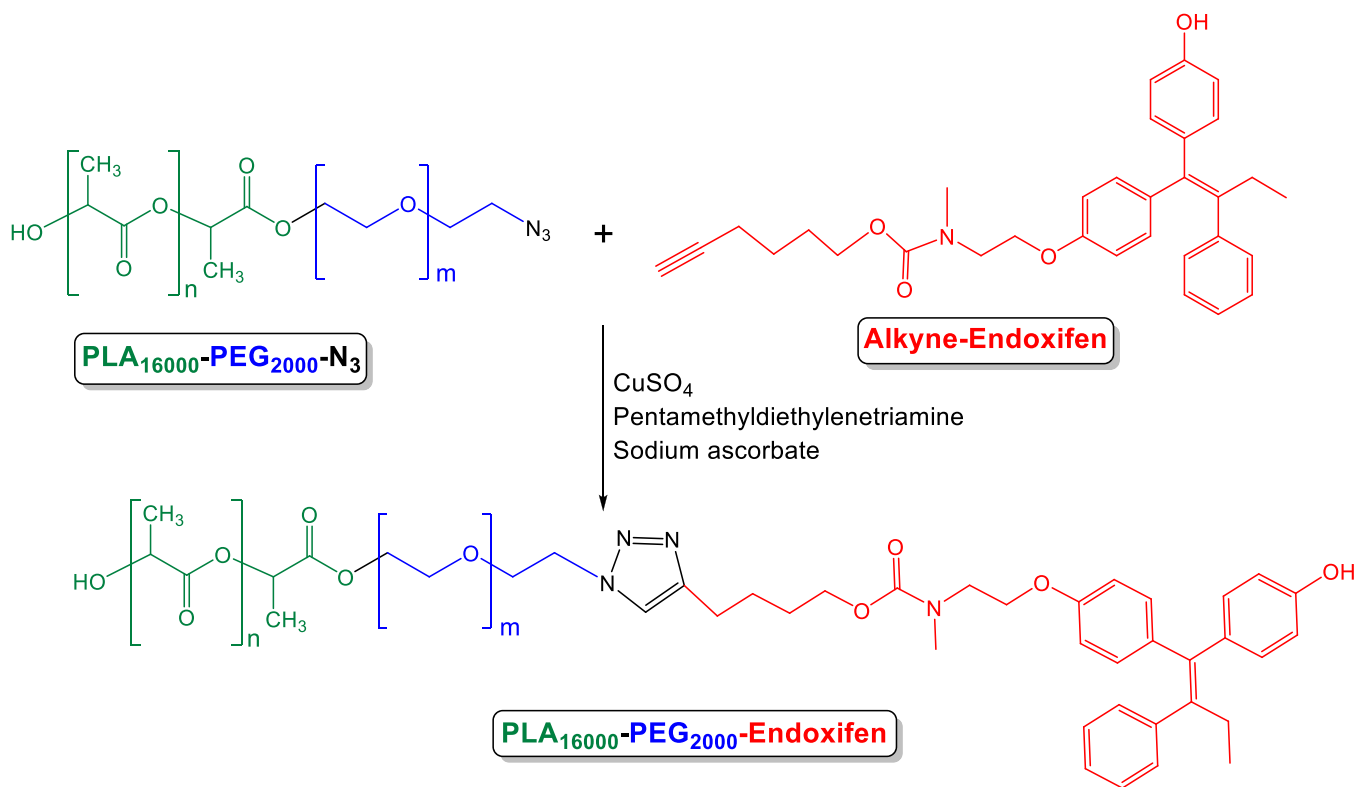
85:10:5 molar ratios of the azobenzene polymer, END-conjugated polymer, and LR dye. A consistent amount of doxorubicin HCl (0.2 mg/mL) was encapsulated into both nontargeted and targeted polymersome samples. Plain, non-targeted, and targeted polymersomes were all prepared according to our previously reported protocols.[12]

2.4. Characterization. Polymersomes were incubated in normoxic (21% O$_2$) and hypoxic (24 h, 2% O$_2$) conditions. A mixture of NADPH (50 μM), human liver microsomes (50 μL), and polymersomes (500 μL) was used to prepare hypoxic samples. An atomic force microscope (AFM, NTEGRA) was used for AFM imaging. The transmission electron microscope (TEM, JOEL JEM-2100) was employed for TEM imaging using both normoxic and hypoxic polymersomes, as previously reported.[12] Dynamic light scattering (DLS, Malvern Zetasizer) was used for determining the charge and size of the polymersomes under hypoxic and normoxic conditions by measuring each sample six times and recording the averages.

2.5. Release Study. A series of DOX concentrations were used to create a calibration curve. The loading content and percent encapsulation of DOX within the vesicles were calculated by measuring the absorbance (480 nm). DOX release from the polymersomes was determined by preparing a combination of targeted nanoparticles, NADPH, human liver microsomes, and HEPES buffer (pH 7.4, 25 mM) within a dialysis membrane (10 kDa molecular weight cut off), based on a reported protocol.[12]
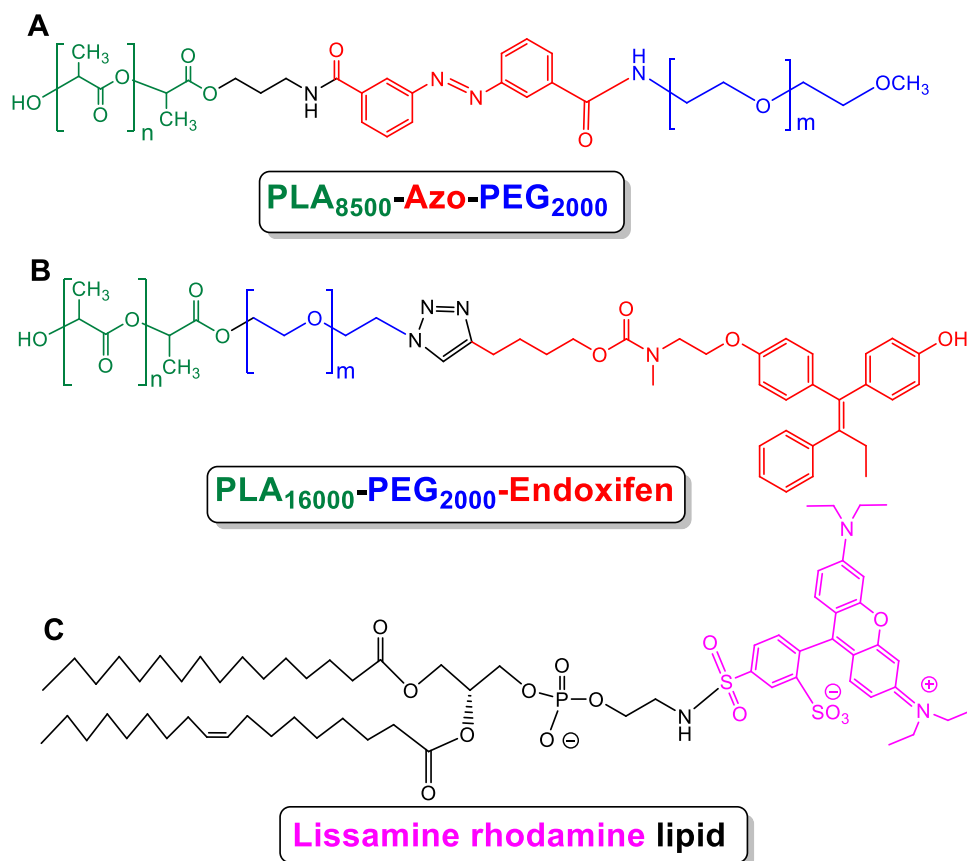
2.6. Cellular Internalization. The MCF7 (ER+) and MDA-MB231 triple-negative (ER−, PR−, HER2−) breast cancer cells were cultured in the DMEM medium containing 10% fetal bovine serum (FBS). The cells (5000/well) were seeded in two cell culture plates and incubated in normoxic (21% O$_2$) and hypoxic (2% O$_2$) conditions overnight. Then,

5.5 μM END and the equivalent amount of nontargeted and targeted buffer-encapsulated nanoparticles and a mixture of 5.5 μM END and END-conjugated nanoparticles were used for treating the cells for 3 h. After washing, the cell nucleus and skeleton were stained with DAPI (Invitrogen) and Phalloidin (Biotium) dyes and then washed again with PBS. The cells were imaged by a 20× objective using a Leica DMi8 fluorescence microscope (Leica Microsystems, Inc.).

2.7. Polymer Toxicity. The cells (5000/well) were cultured in two plates and incubated in normoxia (21% O$_2$) and hypoxia (2% O$_2$) conditions overnight. HEPES buffer-encapsulated END-polymersomes (20−100 μg/mL) were incubated with the cells for 72 h. Then, a 1:9 volume ratio of Alamar Blue to the cell culture medium was incubated with the cells for 5 h. The cytotoxicity was calculated by measuring the fluorescence using an excitation wavelength of 560 nm and an emission wavelength of 595 nm.

2.8. Toxicity of DOX-Polymersomes in Monolayer Cultures. The cells (5000/well) were cultured in two plates and incubated in normoxic (21% O$_2$) and hypoxic (2% O$_2$) conditions overnight. When the cells were 80% confluent, they were divided into four treatments: control (without treatment), free DOX, nontargeted polymersomes (DOX-HRPs), and targeted polymersomes (END-DOX-HRPs). Subsequently, 2, 4, and 8 μM DOX within all doxorubicin-containing formulations were used to treat the cells for 72 h. The plates were then washed with PBS, and the cytotoxicity was calculated using the Alamar Blue assay described in the previous paragraph.

2.9. Spheroid Cytotoxicity Study. The MCF7 cell spheroids were prepared by a NanoShuttle three-dimensional kit (Greiner Bio-One). NanoShuttle-PL magnetic nano-particles (150 μL) were added into an 80% confluent MCF7

Scheme 2. Structures of Synthesized Polymers and Fluorescent Lipid Dye[a]

[a](A) PLA$_{8500}$−Azo−PEG$_{2000}$ polymer, (B) PLA$_{16000}$−PEG$_{2000}$−Endoxifen, and (C) lissamine rhodamine lipid.
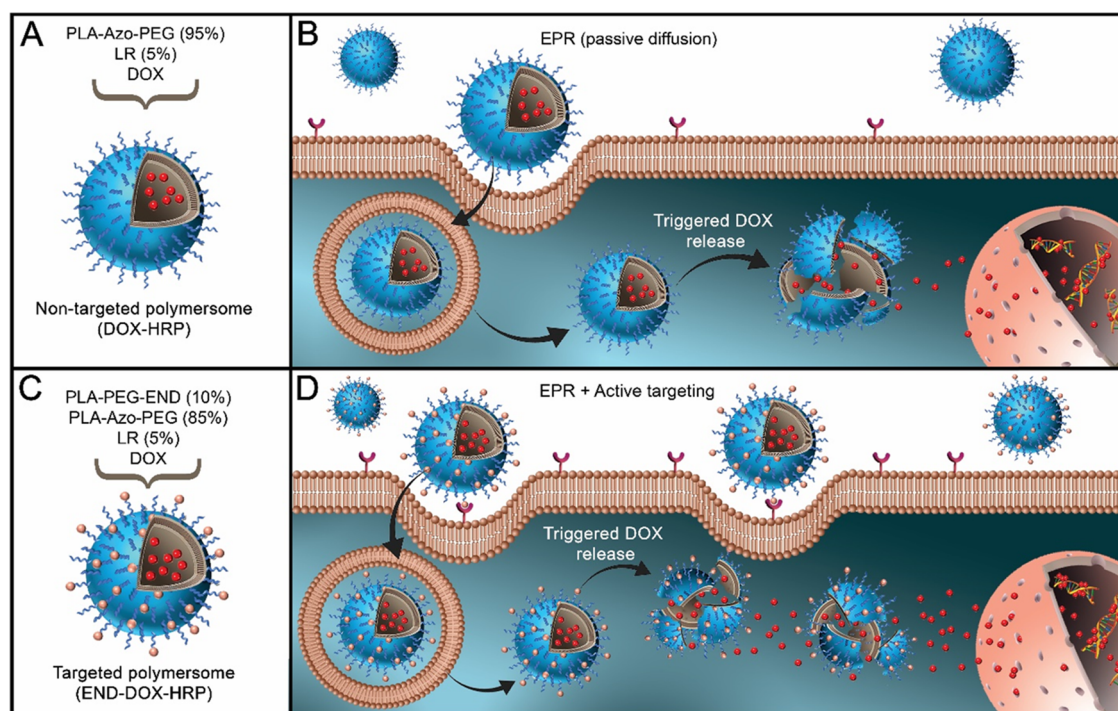
Figure 1. Illustration of nontargeted and targeted polymersomes encapsulating doxorubicin. (A) Components of nontargeted polymersomes. (B) Internalization of nontargeted polymersomes in cancer cells via passive diffusion. (C) Components of targeted polymersomes. (D) Internalization of targeted polymersomes in cancer cells via receptor-mediated endocytosis.

cell culture T-25 flask and incubated 24 h. The flask was washed with PBS, and the cells were then dislodged, counted, and 25 000 cells were added into each well while placing the plates on a spheroid drive for 30 min. The plates were separately incubated in normoxia (21% O_2) and hypoxia (2% O_2) conditions overnight. Subsequently, the cells were incubated with the same four treatments as monolayer cultures and treated with 2, 4, and 8 μM DOX in the formulations for 3 days. The spheroids were washed twice with PBS and the spheroid drives were removed to detach the spheroids. Then, the spheroids were moved into new plates and incubated for 24 h. The cytotoxicity was evaluated by Alamar Blue assay. To further assess the effect of free drug, nontargeted, and targeted polymersomes on the growth of the spheroids, another plate of 6-day-old spheroids was incubated with 8 μM DOX, nontargeted DOX-HRPs, and targeted END-DOX-HRPs for 3 days under normoxic (21% O_2) and hypoxic (2% O_2) conditions. The spheroids were then washed, and their growth was monitored until day 16. The percent growth rate was analyzed by the NIH ImageJ software.

2.10. Statistical Analysis. All statistical analyses were carried out by OriginPro 9.3 (Northampton, Massachusetts), and the results are shown as mean ± SEM. The significant difference among various drug-treated groups in hypoxic and normoxic conditions was evaluated by ANOVA.

3. RESULTS AND DISCUSSION

3.1. Polymer Characterization and Polymersome Preparation. The $PLA_{16000}-PEG_{2000}-Endoxifen$ polymer was synthesized by a cycloaddition reaction between alkyne-endoxifen and $PLA-PEG-N_3$ (Scheme 1). The polymers were characterized by gel permeation chromatography (GPC) and ^{1}H-NMR spectroscopy (Supporting Information, Figures S6 and S7). DOX was encapsulated within the polymersomes. Lissamine rhodamine lipid dye was incorporated into the polymersomes to visualize them through the gel filtration chromatography column and isolate the drug-encapsulated vesicles. The structures of the polymers used in polymersome preparation are shown in Scheme 2. Polymersomes are formed when the molar mass ratio of the hydrophilic part to the total polymer is between 1:5 and 2:5.[50] For our studies, this ratio was 1:5. The surface PEG enhances the systemic half-life of the vesicles in blood circulation.[12] The targeted nanoparticles were optimized to contain 10% PLA−PEG−Endoxifen polymer for efficient interactions with the membrane-associated estrogen receptors on the MCF7 cells.

We developed both nontargeted DOX-encapsulated (DOX-HRPs) and targeted hypoxia-responsive polymersomes (END-DOX-HRPs). These nanoparticles are expected to accumulate within the tumors based on the EPR effect passively.[21] However, the functionalized polymersomes with targeting ligands not only accumulate within the tumor environment via the EPR effect but also selectively interact with the overexpressed surface receptors on cancer cells and enter the cells through active transport (Figure 1).[13,21]

The solvent-exchange procedure was used to prepare the polymersomes[26] and subsequently characterized by DLS, AFM, and TEM imaging. The loading content and average percent encapsulation of doxorubicin within nontargeted and targeted polymersomes were calculated (Table 1). The loading capacity of the polymeric nanoparticles depends on various factors, including the size of polymeric nanoparticles, the molecular weight of the polymer components, and the

Table 1. Encapsulation Efficiency (EE%) and Loading Content (LC%) of the Polymersomes

polymersome	encapsulation efficiency (%)	loading content (%)
nontargeted (DOX-HRP)	46 ± 5	8.1 ± 1.3
targeted (END-DOX-HRP)	68 ± 6	10.2 ± 2.1

preparation methods. The molecular weight of the polymers in this study was 10 500. DOX was loaded into these nanoparticles based on the pH gradient method. In addition, a 10% molar ratio of the endoxifen polymers was used to prepare targeted vesicles. Overall, these factors affected the encapsulation efficiency of these nanoparticles to be around 50% for the nontargeted polymersomes and about 70% for targeted polymersomes. The nanoparticles' average charge and hydrodynamic diameter were measured under hypoxic and normoxic conditions by dynamic light scattering (Figure 2, Table 2). We observed that the average diameter of the DOX-encapsulated targeted polymersomes (164 ± 7 nm) was larger than the nontargeted vesicles (122 ± 5 nm). The increased hydrodynamic diameter is likely due to incorporating the endoxifen-conjugated polymer ($PLA_{16000}-PEG_{2000}-Endoxifen$, Scheme 2) with a higher molecular weight of the PLA block.

We observed that the polymersomes' size changed substantially after exposure to hypoxia (Table 2, Figure 2). It is likely due to disintegration and coalescence to make smaller and larger vesicles with diameter ranges of 40−430 nm for nontargeted and 65−680 nm for targeted polymersomes (Figure 2C,D). Accordingly, the polydispersity indices (PDI) for the polymersomes increased under hypoxia (0.14 ± 0.06 to 0.66 ± 0.17 for nontargeted; 0.15 ± 0.05 to 0.73 ± 0.16 for targeted; Table 2). TEM and AFM images corroborated these observations (Figure 3). The hypoxic tumor microenvironment is enriched in reductase enzymes.[51] For the *in vitro* studies, we simulated the reductive microenvironment with human liver microsomes (source of reductase enzymes) and NADPH (for enzyme activity).[12] Under hypoxia, reduction of the diazo linker of the hypoxia-responsive polymer separates the hydrophobic PLA and hydrophilic PEG blocks (Figure 2E).[11,52,53] The resultant structural collapse of the polymersomes facilitates the release of the encapsulated doxorubicin.[12] Due to the high metabolism, impaired blood supply, and low oxygen concentration within the tumors, cancer cells undergo glycolysis to produce pyruvate, making the hypoxic tumor regions more acidic. The reduction of azobenzene (−N═N−) to hydrazobenzene (−NH−NH−) under acidic conditions occurs at −0.20 V, and the reduction of hydrazobenzene to PLA− and PEG−amine occurs at −0.40 V.[54] Based on a study related to the measurement of the intracellular redox potential of the cancer cells, this value was reported to be around −390 to −420 mV after inducing the hypoxia.[55] The more negative intracellular reduction potential value compared to the reduction potential of the azobenzene indicates that intracellular agents act as the reducers to donate electrons to the azobenzene linker for breaking the nitrogen−nitrogen bonds and release the encapsulated drugs within the cell. The ζ-potential was positive under both normoxic and hypoxic conditions.

3.2. Doxorubicin Release from Polymersomes. To assess drug release from the polymersomes under hypoxic conditions, DOX was encapsulated into the END-conjugated
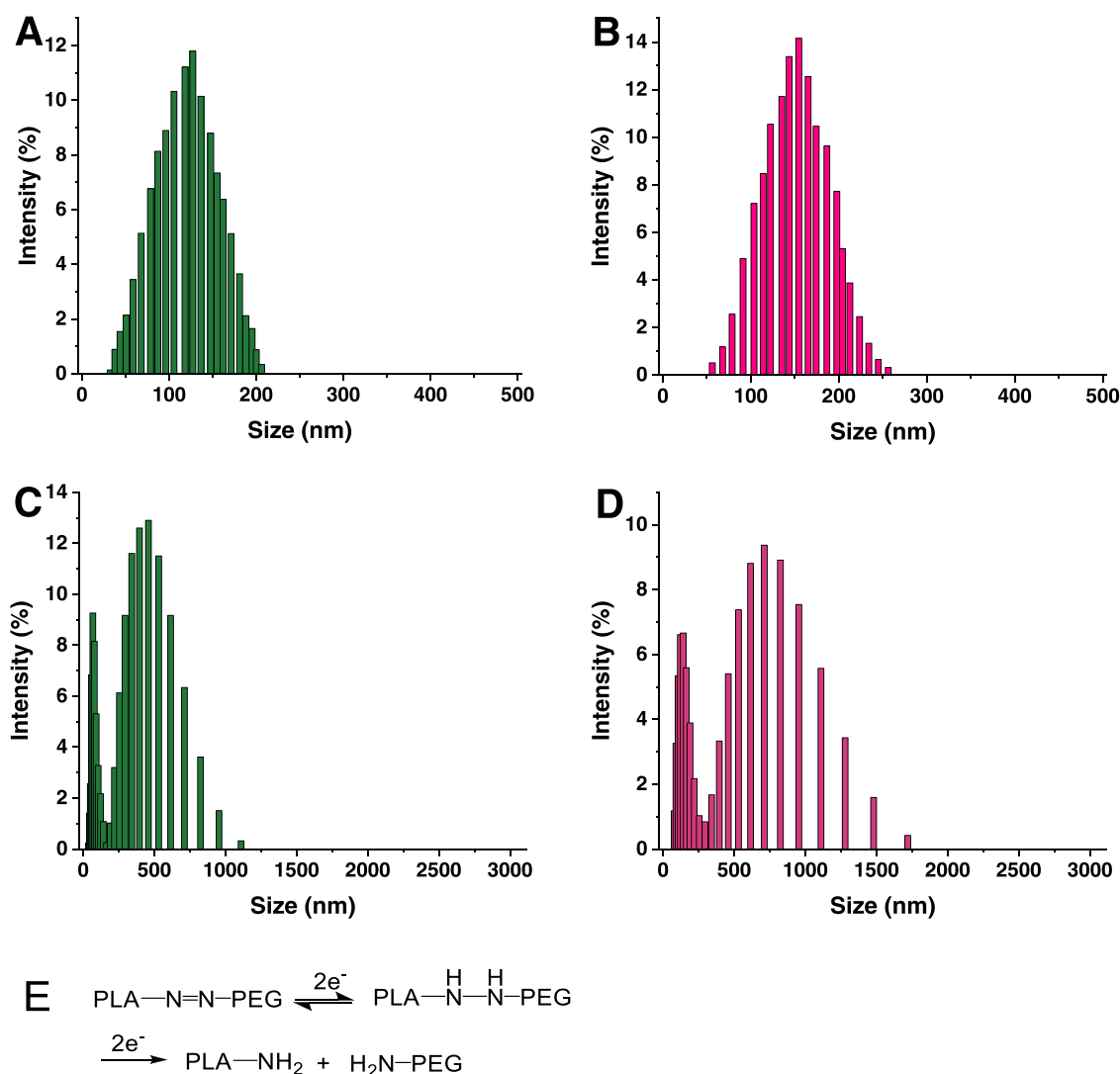
Figure 2. (A) Hydrodynamic diameter of nontargeted polymersomes under normoxia. (B) Hydrodynamic diameter of targeted polymersomes under normoxia. (C) Hydrodynamic diameter of nontargeted polymersomes under hypoxia. (D) Hydrodynamic diameter of targeted polymersomes under hypoxia. (E) Proposed mechanism of drug release under hypoxia in the presence of reducing agents.

Table 2. Average Hydrodynamic Diameter, ζ-Potential, and Polydispersity Index (PDI) of the DOX-Encapsulated Polymersomes

	average diameter (nm)		ζ-potential (mV)		PDI	
polymersome	normoxia	hypoxia	normoxia	hypoxia	normoxia	hypoxia
nontargeted	122 ± 5	41 ± 6, 425 ± 8	0.18 ± 0.03	0.32 ± 0.14	0.14 ± 0.06	0.66 ± 0.17
targeted	164 ± 7	68 ± 8, 678 ± 9	0.27 ± 0.19	0.44 ± 0.18	0.15 ± 0.05	0.73 ± 0.16

nanoparticles. These polymersomes were incubated under hypoxia (human liver microsomes, NADPH, 2% oxygen) and normoxia (human liver microsomes, NADPH, 21% oxygen), and drug release was monitored for 12 h (Figure 4).

We observed higher DOX release from the polymersomes under hypoxia compared to normoxia conditions. Polymersomes released more than 96% of their cargo under hypoxia conditions within 12 h. However, less than 27% of DOX encapsulated in polymersomes was released in normoxia conditions during the same time. The results indicated that reducing the hypoxia-responsive azobenzene linker leads to the release of the encapsulated drug under hypoxia conditions. We also decreased the oxygen level to 1 and 0.1% and performed DOX release under hypoxia conditions. The results of this

study demonstrated that over 97% of the drug was released from the polymersomes under both 1 and 0.1% oxygen but in a shorter time compared to 2% oxygen (Supporting Information, Figure S8). This might be due to the facilitated enzymatic reaction to break the hypoxia-responsive azobenzene linker and disintegrate the polymeric vesicles. TEM and AFM images demonstrated that polymersomes maintained their standard shape under normoxia conditions while disrupting their vesicular structure under hypoxia conditions (Figure 3).

3.3. Cellular Internalization. To evaluate cellular internalization, the ER+ breast cancer cells (MCF7) were treated with 5.5 μM free END, equivalent amounts of nontargeted and targeted buffer-encapsulated nanoparticles, and a mixture of 5.5 μM END and END-conjugated polymersomes under
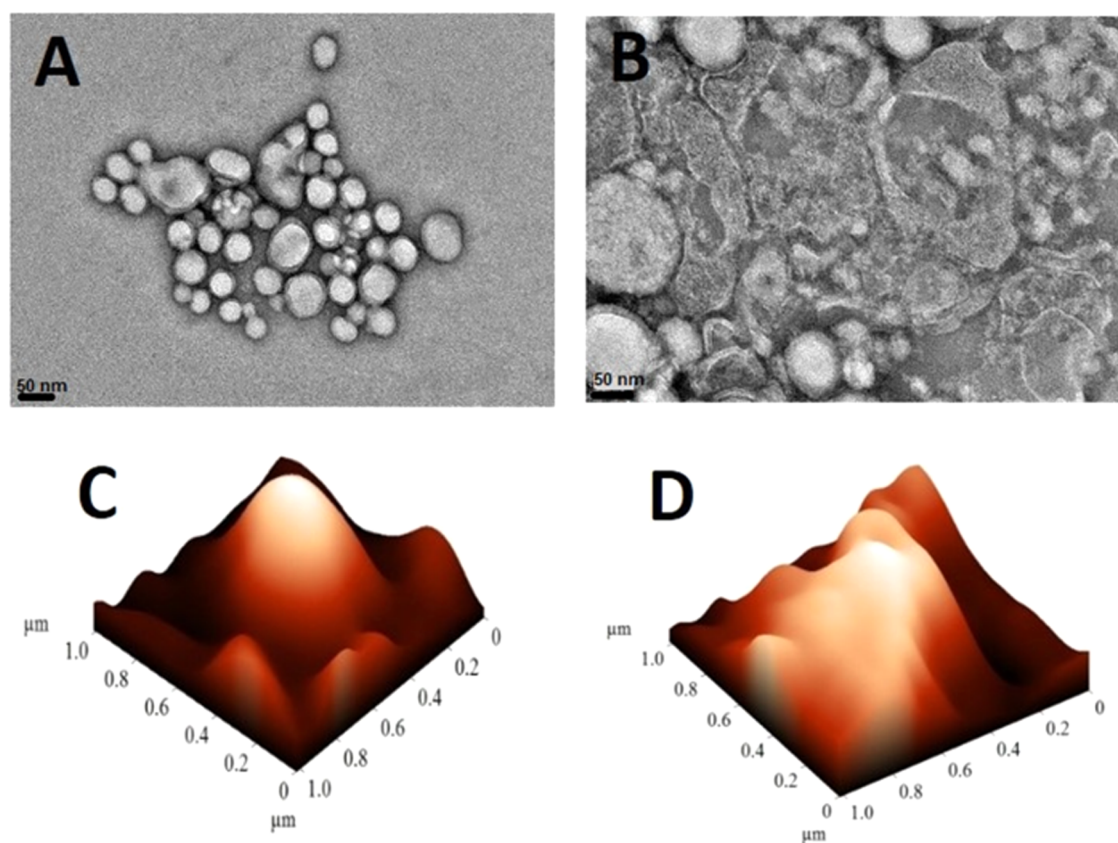
Figure 3. TEM and AFM images of endoxifen-polymersomes under normoxic (A, C) and hypoxic conditions (B, D).
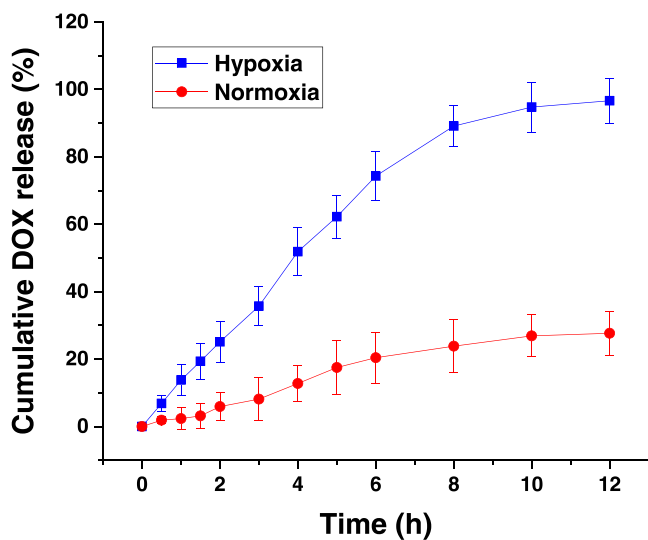

Figure 4. Cumulative release of doxorubicin from targeted hypoxia-responsive nanoparticles in hypoxic (2% oxygen) and normoxic (21% oxygen) conditions ($n = 3$).

hypoxia and normoxia conditions for 3 h. Lissamine rhodamine dye was incorporated into the polymersome bilayer to follow the cellular uptake using a fluorescence microscope (Figure 5A,B).[12] The fluorescence density of the images was normalized based on the number of breast cancer cells. NIH ImageJ was used to calculate all treatment groups' fluorescence intensity under hypoxic and normoxic conditions (Figure 5C).

It was observed that targeted END-conjugated polymer-somes entered the breast cancer cells under both normoxia and

hypoxia conditions due to ligand−receptor interaction between endoxifen and estrogen receptors (enlargement within Figure 5A,B). The image density of targeted polymersomes within the cells in both normoxia and hypoxia conditions was higher than the combination of targeted polymersomes and END treatment ($p < 0.05$) and higher than nontargeted polymersomes ($p < 0.01$). We also observed that targeted polymersomes' fluorescence density was 7.8 and 6 times higher than nontargeted polymersome-treated groups in hypoxia and normoxia conditions. The fluorescence density in targeted polymersomes in hypoxia conditions was also higher than normoxia conditions ($p < 0.01$).

Various factors control the retention of nanoparticles inside cancer cells, such as the size, concentration, duration of cellular exposure to hypoxia, and uptake or efflux of the nanovesicles from the cells. According to a recent study, nanoparticles' entry into MDA-MB-231 breast cancer cells increases under hypoxia conditions compared to normoxia conditions.[56] Another study indicated an enhanced internalization of gold nanoparticles into the hypoxic MCF7 cells.[57] In the current study, we observed that exposing the ER+ MCF7 cells to hypoxia conditions for 3 h led to enhanced uptake of the targeted endoxifen-conjugated polymersomes (Figure 5B). In addition, it was observed that targeted END-polymersomes internalize more to the cancer cells compared to nontargeted vesicles (Figure 5), likely due to the overexpression of membrane-bound estrogen receptors on the surface of breast cancer cells.[44] To evaluate the potency of END-polymersomes, we also treated the ER+ MCF7 cells with free END and a combination of END-polymersomes and free END. We observed that free END had minor entry to the cells. However, when we treated the cells with a combination of free END and
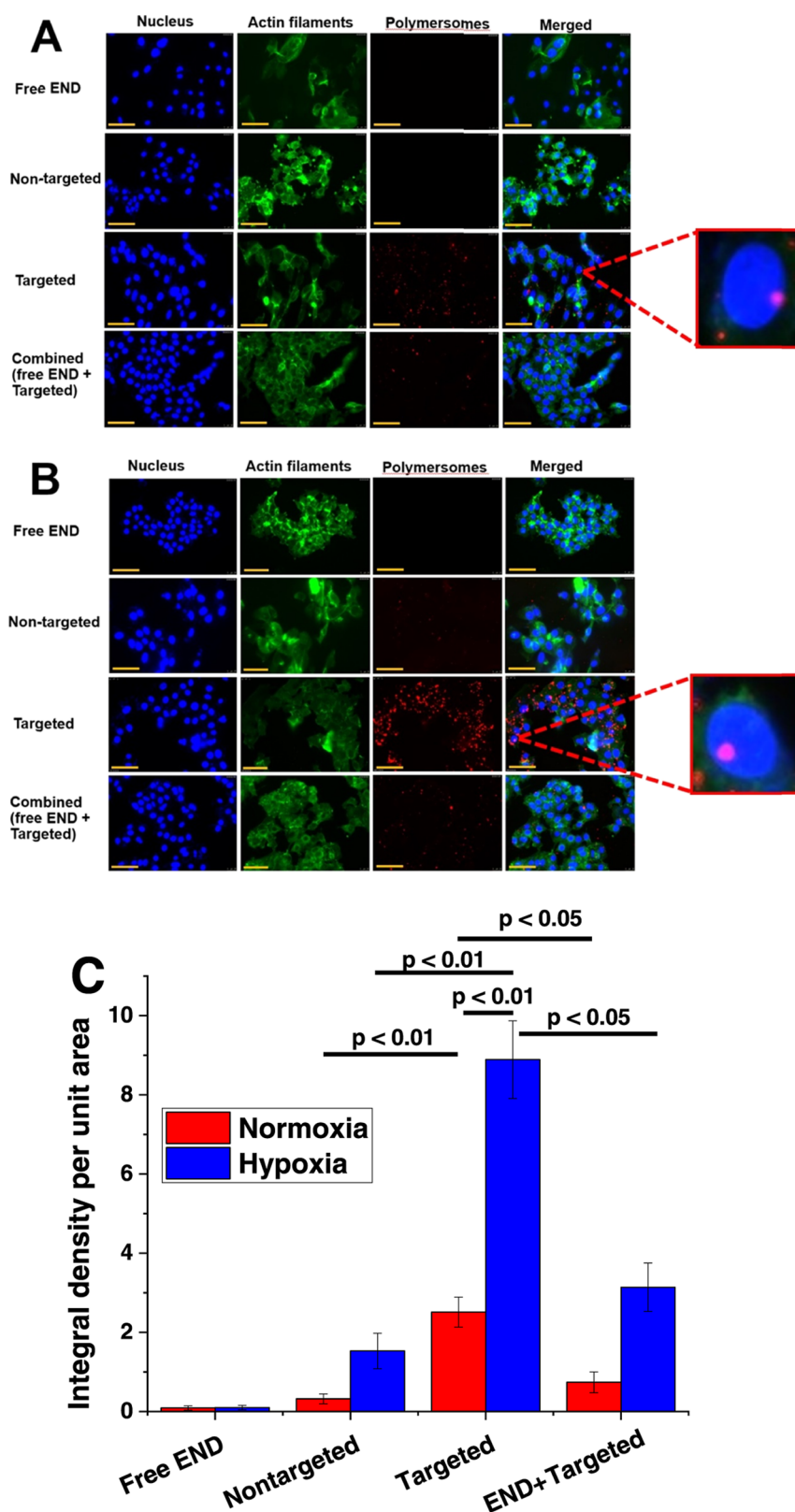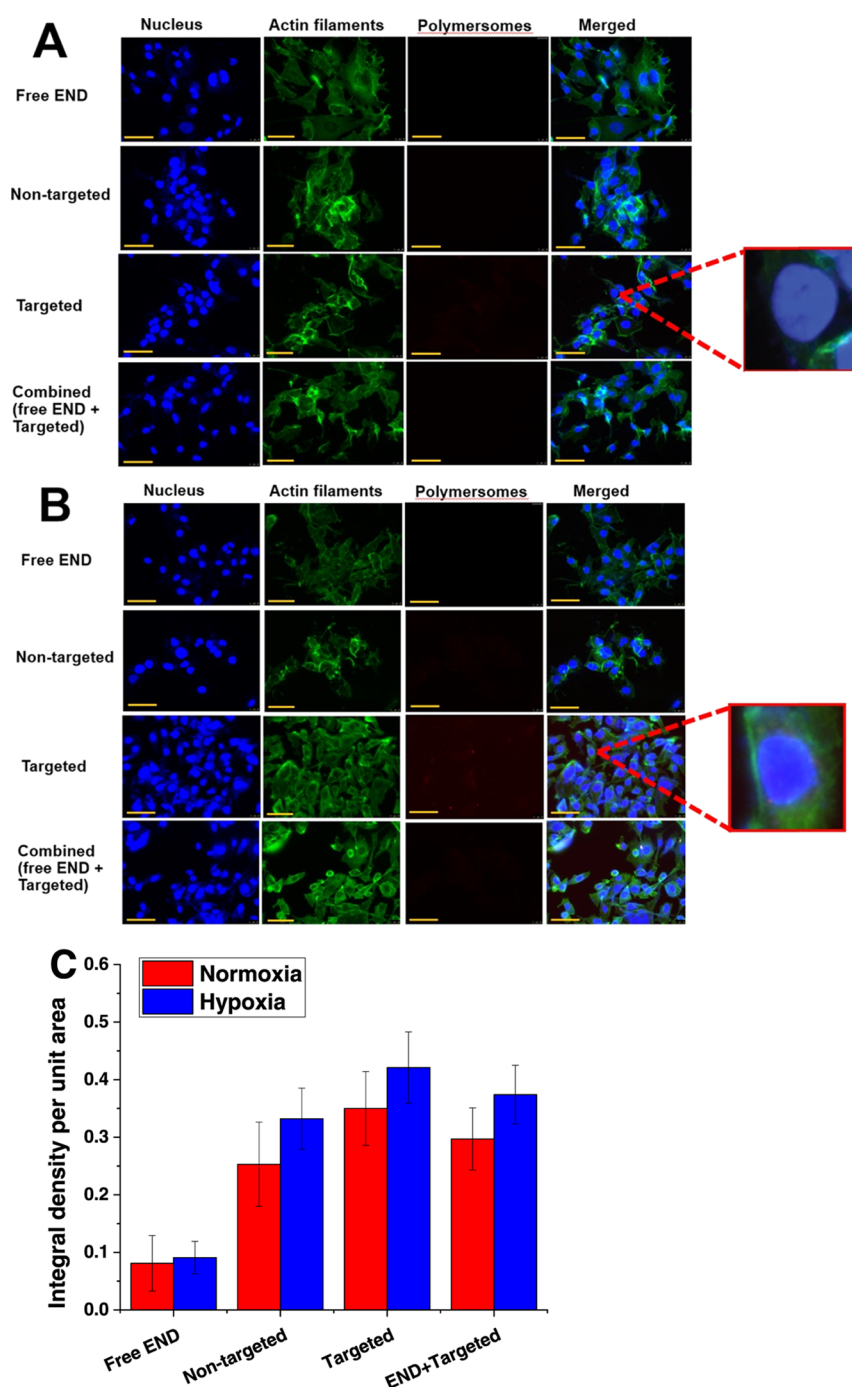
Figure 5. Fluorescence images of cellular uptake of free endoxifen (free END), nontargeted and targeted polymersomes, and a combination of END and targeted polymersomes in MCF7 cells after 3 h under normoxia (A) and hypoxia (B) conditions (scale bar: 50 μm). The enlargements (100×) show the presence of the polymersomes inside the cell nuclei. (C) Quantitative fluorescence intensity of the cells under normoxia and hypoxia conditions ($n = 3$).

targeted END-polymersomes, free END inhibited END-polymersomes' internalization. The free END binds to the

estrogen receptor and competitively inhibits END-polymersomes from interacting with the receptors.

Figure 6. Fluorescence images of cellular uptake of free endoxifen (free END), nontargeted and targeted polymersomes, and a combination of END and targeted polymersomes on triple-negative breast cancer cells MDA-MB-231 after 3 h under normoxia (A) and hypoxia (B) conditions (scale bar: 50 μm). (C) Quantitative fluorescence intensity of the cells in normoxia and hypoxia conditions ($n = 3$).

To further probe the role of ER in cellular internalization, we incubated the triple-negative breast cancer cells (MDA-MB-231) with the same polymersome formulations and imaged them using a fluorescence microscope (Figure 6A,B). We observed a weak fluorescence intensity from both targeted and nontargeted polymersomes and no nuclear localization. Moreover, the intensities were not significantly different in hypoxia ($p = 0.124$) and normoxia ($p = 0.251$) conditions and the absence and presence of added endoxifen (Figure 6C). Due to the lack of estrogen receptors on the surface of MDA-MB-231 cells,[14] endoxifen could not affect the nanoparticle

uptake when the cells were incubated with a combination of END-polymersomes and free END (Figure 6C).

3.4. Cytotoxicity in Monolayer and Spheroid Cultures. To evaluate the toxicity, MCF7 cells were incubated with different concentrations of buffer-encapsulated END-polymersomes for 3 days. The cells were more than 85% viable with the highest polymer concentration (100 μg/mL) tested in normoxia and hypoxia conditions (Figure 7). For the subsequent experiments, we used 1 mg/mL of the total polymer in preparing the polymersomes. To determine the efficacy of DOX-loaded polymersomes, the MCF7 monolayer
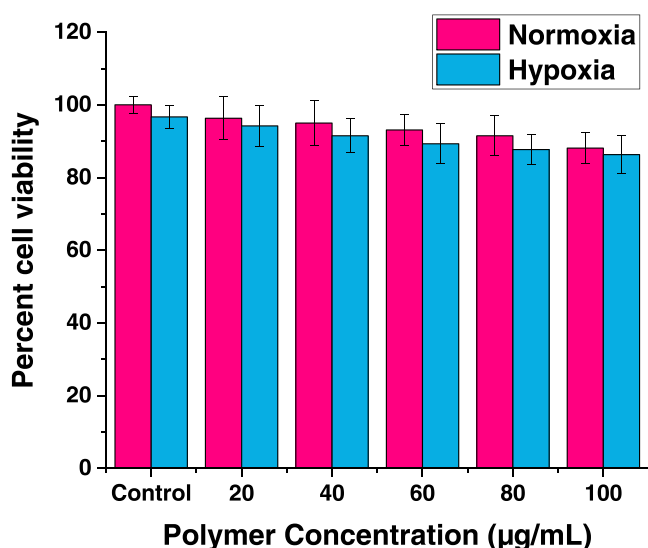
Figure 7. Toxicity of buffer-encapsulated endoxifen-conjugated polymersomes on MCF7 breast cancer cells under normoxic and hypoxic conditions (72 h, $n = 3$).

and three-dimensional spheroid cell cultures were incubated for 72 h with four treatments: nontargeted nanoparticles (DOX-HRPs), targeted END-conjugated nanoparticles (END-DOX-HRPs), control (buffer only), and free DOX (Figure 8A,B).

The MCF7 cells were treated with various DOX concentrations (1−15 μM). The minimum drug concentration with significant differences between the treated and control cells was 8 μM. It was observed that treating the MCF7 monolayer and spheroid cultures under hypoxia conditions with nontargeted polymersomes (DOX-HRPs; [DOX] = 8 μM) reduced the cell viability to 50 and 65%, respectively. The reduced cell viability is likely due to passive diffusion of the polymersomes inside the breast cancer cells and subsequent release of doxorubicin in the reducing microenvironment of the cytosol.[58] However, treating the monolayer and spheroids under hypoxia conditions with the targeted polymersomes (END-DOX-HRPs; [DOX] = 8 μM) decreased the viability of the cells to 18 and 31%, respectively. The targeted nanoparticles show higher cellular internalization compared to the nontargeted counterparts, and this effect is enhanced in hypoxia conditions (Figure 5). Hence, the higher cell death with the targeted polymersomes in hypoxia conditions is likely due to more efficient internalization and subsequent DOX release. However, for the experiments under hypoxia conditions, we cannot rule out some DOX release from the vesicles outside the cells, followed by the passive diffusion of the drug in the cytosol.

The cell viability in treated microtumor-like spheroid cultures was higher than that in the monolayer, possibly due to the spheroids' dense structure. A significant difference ($p < 0.05$) was shown between hypoxia and normoxia conditions when the monolayer and spheroid cultures were incubated with targeted polymersomes. Under hypoxia conditions, targeted polymersomes decreased the monolayer and spheroid cultures' viability to 18 and 31%, respectively (Figure 8A,B, brown bars). We also observed a significant difference ($p < 0.05$) between targeted and nontargeted treatment groups under hypoxia conditions in both monolayer and spheroid cell cultures (Figure 8A,B, purple and brown bars), likely for the

enhanced targeted receptor-mediated cellular uptake.[10] There was a significant difference ($p < 0.05$) between hypoxia and normoxia conditions only in monolayer cultures for the nontargeted treatment group (Figure 8A, green and purple bars). The cell viability decreased to 30% between these two groups. Hypoxia conditions would release more DOX from the vesicles, leading to increased cell death. In the spheroids, this effect is not pronounced, likely due to the lack of efficient diffusion of the released drug through the dense cluster of the cells.

The polymersomes release 35% of their cargo within 3 h and 90% after 8 h in hypoxia conditions (Figure 4). This ensures that 72 h treatment is enough for the vesicles to pass through the cancer cells, disintegrate, and release the encapsulated DOX. According to the EPR effect (passive diffusion), both nontargeted and targeted polymersomes can accumulate into the tumor.[21] However, in addition to passive diffusion, targeted vesicles demonstrate enhanced cellular uptake and toxicity due to estrogen receptor-mediated endocytosis. The overexpressed estrogen receptors on the MCF7 cells[44] contribute to increased receptor-mediated nanoparticle internalization. We note that hypoxia does not induce the expression of membrane-associated estrogen receptors on MCF7 cells.[59] However, hypoxia conditions would release more DOX from the vesicles.

To further estimate the polymersomes' efficacy, the 6-day-old spheroids were treated with 8 μM free DOX, nontargeted, and targeted nanoparticles for 72 h in hypoxia and normoxia conditions, and their growth was monitored for 16 days (Figure 8C−E). We observed changes in the spheroid volume compared to the beginning of the treatment. For instance, the size of the control spheroids (buffer treatment) increased by about 2.5-fold (250%) by day 16 (Figure 8C,D, black squares). The targeted polymersomes were more toxic toward breast cancer cells in hypoxia conditions by shrinking the spheroid volume up to 73% (Figure 8C, green inverted triangles). In comparison, nontargeted polymersomes reduced this volume by 32% in hypoxia conditions (Figure 8C, blue triangles). The spheroid growth curve results in hypoxia conditions corroborate the higher toxicity of targeted polymersomes than nontargeted vesicles (Figure 8B). We also observed that targeted polymersomes in normoxia conditions decreased the spheroid volume up to 52% (Figure 8D, green inverted triangles), while nontargeted polymersomes only shrink this volume by 20% (Figure 8D, blue triangles). The targeted polymersomes enter the MCF7 cells more easily than the nontargeted vesicles due to endoxifen's interactions on the polymersomes and the estrogen receptors on the cell surface. In addition, targeted polymersomes significantly decreased the volume of spheroids compared to free DOX ($p < 0.05$), nontargeted polymersomes ($p < 0.05$), and the control group ($p < 0.01$) in hypoxia conditions (Figure 8C). Overall, we observed that targeted polymersomes are more potent in shrinking breast microtumors than nontargeted polymersomes and control groups in hypoxia and normoxia conditions. However, the effect was more pronounced under hypoxia conditions.

4. CONCLUSIONS

The END-decorated doxorubicin-encapsulated polymersomes described in this study are targeted polymeric hypoxia-responsive nanoparticles for drug delivery to ER+ breast microtumors. They selectively bind to overexpressed ERs on the surface of breast cancer cells with the aid of surface-
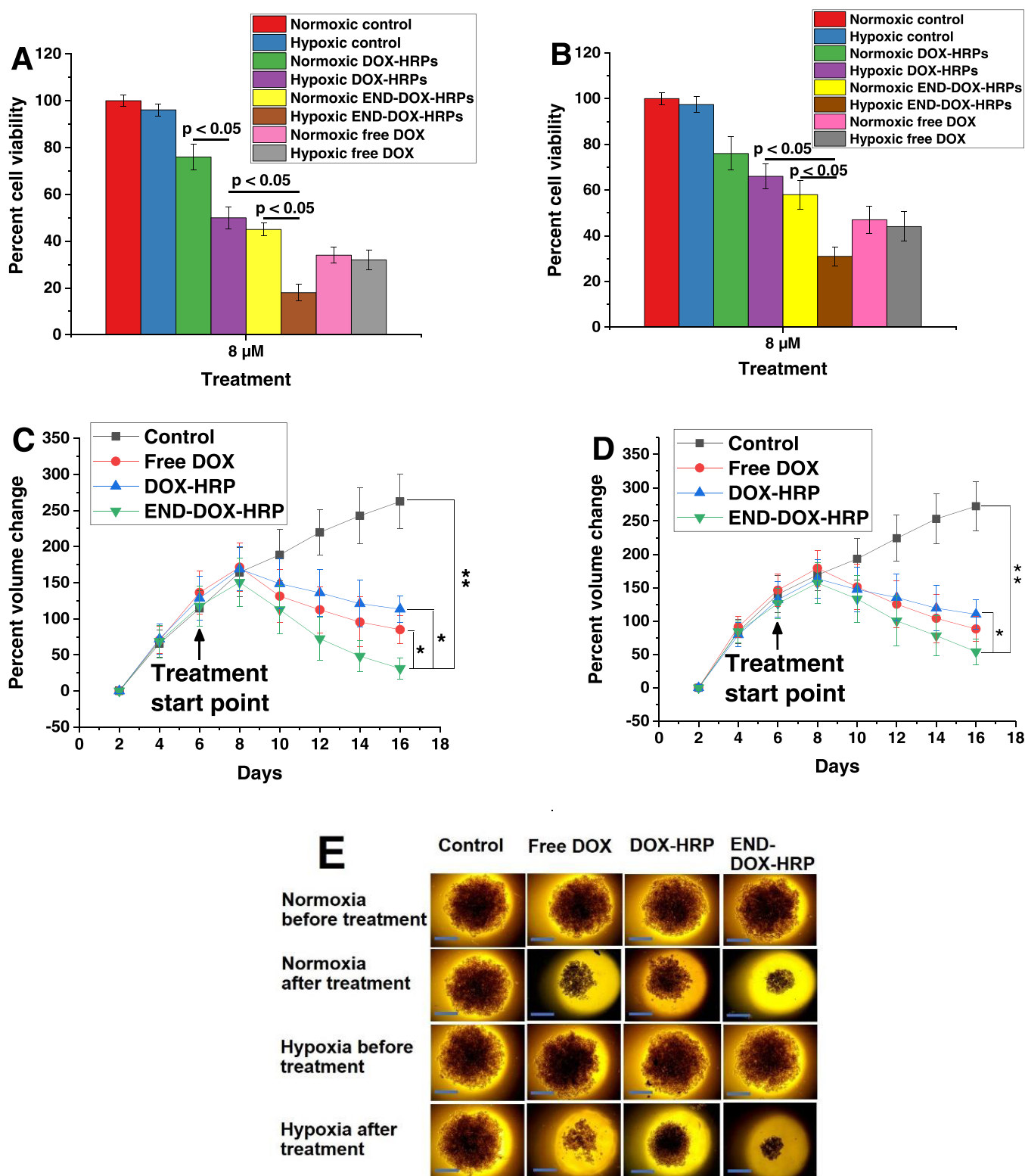
Figure 8. Viability of MCF7 cells under normoxia and hypoxia conditions after 72 h treatment in the monolayer (A) and three-dimensional spheroid cultures (B) ($n = 3$, $p < 0.05$). Growth curves of MCF7 spheroid cultures in hypoxia (C) and normoxia (D) conditions ($n = 3$, **$p < 0.01$, *$p < 0.05$). (E) MCF7 spheroids under normoxia and hypoxia conditions before and after the treatment with DOX-encapsulated nanoparticles and free DOX (scale bar: 100 μm).

anchored END molecules and enter the cytosol. In addition, they release the anticancer drug in hypoxia conditions due to the presence of the hypoxia-responsive diazobenzene moieties. We note that some drug release from the nanocarriers can occur in the extracellular matrix also in hypoxia conditions.

Under hypoxia conditions, targeted polymersomes demonstrated higher cytotoxicity on the ER+ breast cancer monolayer and spheroid cultures than nontargeted polymersomes and free drugs. In addition, targeted polymersomes shrank the breast microtumor volume more efficiently than nontargeted

polymersomes in hypoxia and normoxia conditions. Based on our literature survey, this is the first report of using endoxifen to target ER+ breast cancer cells by polymer nanoparticles. Overall, our targeted polymersomes' merits are the ability to interact with estrogen receptors specifically, disintegrate in the cancer cells under low oxygen partial pressure, selectively release their encapsulated drug in hypoxic breast cancer microtumors, diminish the cancer cell viability, and enhance the therapeutic efficacy of an anticancer drug. With further developments, targeted END-conjugated DOX-loaded nanoparticles can deliver chemotherapeutic drugs and treat breast cancer.

■ ASSOCIATED CONTENT

Ⓢ Supporting Information

The Supporting Information is available free of charge at https://pubs.acs.org/doi/10.1021/acsomega.1c02250.

> ^{1}H, ^{13}C NMR spectra, GPC of the synthesized polymers, and doxorubicin release from the polymersomes under 1 and 0.1% oxygen (PDF)

■ AUTHOR INFORMATION

Corresponding Author

Sanku Mallik − *Department of Pharmaceutical Sciences, North Dakota State University, Fargo, North Dakota 58102, United States;* ⓞ orcid.org/0000-0003-4236-2512; Phone: 701-231-7888; Email: Sanku.Mallik@ndsu.edu; Fax: 701-231-7831

Authors

Babak Mamnoon − *Department of Pharmaceutical Sciences, North Dakota State University, Fargo, North Dakota 58102, United States*

Li Feng − *Department of Pharmaceutical Sciences, North Dakota State University, Fargo, North Dakota 58102, United States*

Jamie Froberg − *Department of Physics, North Dakota State University, Fargo, North Dakota 58102, United States*

Yongki Choi − *Department of Physics, North Dakota State University, Fargo, North Dakota 58102, United States;* ⓞ orcid.org/0000-0001-8890-8344

Venkatachalem Sathish − *Department of Pharmaceutical Sciences, North Dakota State University, Fargo, North Dakota 58102, United States*

Oleh Taratula − *Department of Pharmaceutical Sciences, College of Pharmacy, Oregon State University, Portland, Oregon 97201, United States;* ⓞ orcid.org/0000-0002-6227-9110

Olena Taratula − *Department of Pharmaceutical Sciences, College of Pharmacy, Oregon State University, Portland, Oregon 97201, United States*

Complete contact information is available at:
https://pubs.acs.org/10.1021/acsomega.1c02250

Notes

The authors declare no competing financial interest.

■ ACKNOWLEDGMENTS

■ REFERENCES

(1) Müller, A.; Homey, B.; Soto, H.; Ge, N.; Catron, D.; Buchanan, M. E.; McClanahan, T.; Murphy, E.; Yuan, W.; Wagner, S. N.; Barrera, J. L.; Mohar, A.; Verástegui, E.; Zlotnik, A. Involvement of Chemokine Receptors in Breast Cancer Metastasis. *Nature* **2001**, *410*, 50−56.

(2) Pérez-Herrero, E.; Fernández-Medarde, A. Advanced Targeted Therapies in Cancer: Drug Nanocarriers, the Future of Chemotherapy. *Eur. J. Pharm. Biopharm.* **2015**, *93*, 52−79.

(3) Keklikoglou, I.; Cianciaruso, C.; Güç, E.; Squadrito, M. L.; Spring, L. M.; Tazzyman, S.; Lambein, L.; Poissonnier, A.; Ferraro, G. B.; Baer, C.; Cassará, A.; Guichard, A.; Iruela-Arispe, M. L.; Lewis, C. E.; Coussens, L. M.; Bardia, A.; Jain, R. K.; Pollard, J. W.; De Palma, M. Chemotherapy Elicits Pro-Metastatic Extracellular Vesicles in Breast Cancer Models. *Nat. Cell Biol.* **2019**, *21*, 190−202.

(4) Liu, H.; Lee, J. I.; Ahn, T.-G. Effect of Quercetin on the Anti-Tumor Activity of Cisplatin in EMT6 Breast Tumor-Bearing Mice. *Obstet. Gynecol. Sci.* **2019**, *62*, 242−248.

(5) Vakilinezhad, M. A.; Amini, A.; Dara, T.; Alipour, S. Methotrexate and Curcumin Co-Encapsulated PLGA Nanoparticles as a Potential Breast Cancer Therapeutic System: In Vitro and in Vivo Evaluation. *Colloids Surf., B* **2019**, *184*, No. 110515.

(6) Cai, F.; Luis, M. A. F.; Lin, X.; Wang, M.; Cai, L.; Cen, C.; Biskup, E. Anthracycline-Induced Cardiotoxicity in the Chemotherapy Treatment of Breast Cancer: Preventive Strategies and Treatment. *Mol. Clin. Oncol.* **2019**, *11*, 15−23.

(7) Perumalsamy, H.; Sankarapandian, K.; Kandaswamy, N.; Balusamy, S. R.; Periyathambi, D.; Raveendiran, N. Cellular Effect of Styrene Substituted Biscoumarin Caused Cellular Apoptosis and Cell Cycle Arrest in Human Breast Cancer Cells. *Int. J. Biochem. Cell Biol.* **2017**, *92*, 104−114.

(8) Orive, G.; Hernández, R. M.; Gascón, A. R.; Domínguez-Gil, A.; Pedraz, J. L. Drug Delivery in Biotechnology: Present and Future. *Curr. Opin. Biotechnol.* **2003**, *14*, 659−664.

(9) Xu, J.; Zhao, Q.; Jin, Y.; Qiu, L. High Loading of Hydrophilic/Hydrophobic Doxorubicin into Polyphosphazene Polymersome for Breast Cancer Therapy. *Nanomedicine* **2014**, *10*, 349−358.

(10) Confeld, M. I.; Mamnoon, B.; Feng, L.; Jensen-Smith, H.; Ray, P.; Froberg, J.; Kim, J.; Hollingsworth, M. A.; Quadir, M.; Choi, Y.; Mallik, S. Targeting the Tumor Core: Hypoxia-Responsive Nanoparticles for the Delivery of Chemotherapy to Pancreatic Tumors. *Mol. Pharmaceutics* **2020**, *17*, 2849−2863.

(11) Kulkarni, P.; Haldar, M. K.; You, S.; Choi, Y.; Mallik, S. Hypoxia-Responsive Polymersomes for Drug Delivery to Hypoxic Pancreatic Cancer Cells. *Biomacromolecules* **2016**, *17*, 2507−2513.

(12) Mamnoon, B.; Feng, L.; Froberg, J.; Choi, Y.; Sathish, V.; Mallik, S. Hypoxia-Responsive, Polymeric Nanocarriers for Targeted Drug Delivery to Estrogen Receptor-Positive Breast Cancer Cell Spheroids. *Mol. Pharmaceutics* **2020**, *17*, 4312−4322.

(13) Thambi, T.; Deepagan, V. G.; Yoon, H. Y.; Han, H. S.; Kim, S.-H.; Son, S.; Jo, D.-G.; Ahn, C.-H.; Suh, Y. D.; Kim, K.; Chan Kwon, I.; Lee, D. S.; Park, J. H. Hypoxia-Responsive Polymeric Nanoparticles for Tumor-Targeted Drug Delivery. *Biomaterials* **2014**, *35*, 1735−1743.

(14) Mamnoon, B.; Loganathan, J.; Confeld, M. I.; De Fonseka, N.; Feng, L.; Froberg, J.; Choi, Y.; Tuvin, D. M.; Sathish, V.; Mallik, S. Targeted Polymeric Nanoparticles for Drug Delivery to Hypoxic, Triple-Negative Breast Tumors. *ACS Appl. Bio Mater.* **2021**, 1450−1460.

(15) Wilson, W. R.; Hay, M. P. Targeting Hypoxia in Cancer Therapy. *Nat. Rev. Cancer* **2011**, *11*, 393−410.

(16) Alhalhooly, L.; Mamnoon, B.; Kim, J.; Mallik, S.; Choi, Y. Dynamic Cellular Biomechanics in Responses to Chemotherapeutic

Drug in Hypoxia Probed by Atomic Force Spectroscopy. *Oncotarget* **2021**, *12*, 1165−1177.

(17) Peer, D.; Karp, J. M.; Hong, S.; Farokhzad, O. C.; Margalit, R.; Langer, R. Nanocarriers as an Emerging Platform for Cancer Therapy. *Nat. Nanotechnol.* **2007**, *2*, 751−760.

(18) Shi, J.; Votruba, A. R.; Farokhzad, O. C.; Langer, R. Nanotechnology in Drug Delivery and Tissue Engineering: From Discovery to Applications. *Nano Lett.* **2010**, *10*, 3223−3230.

(19) Kearney, C. J.; Mooney, D. J. Macroscale Delivery Systems for Molecular and Cellular Payloads. *Nat. Mater.* **2013**, *12*, 1004−1017.

(20) Cuenca, A. G.; Jiang, H.; Hochwald, S. N.; Delano, M.; Cance, W. G.; Grobmyer, S. R. Emerging Implications of Nanotechnology on Cancer Diagnostics and Therapeutics. *Cancer* **2006**, *107*, 459−466.

(21) Shi, J.; Kantoff, P. W.; Wooster, R.; Farokhzad, O. C. Cancer Nanomedicine: Progress, Challenges and Opportunities. *Nat. Rev. Cancer* **2017**, *17*, 20−37.

(22) Davis, M. E.; Chen, Z. G.; Shin, D. M. Nanoparticle Therapeutics: An Emerging Treatment Modality for Cancer. *Nat. Rev. Drug Discovery* **2008**, *7*, 771−782.

(23) Pullan, J. E.; Mamnoon, B.; Kale, N.; Mallik, S. Chapter 10 - Nanoparticles for Delivering Natural Product Chemotherapeutics to Breast Cancer Cells. In *Discovery and Development of Anti-Breast Cancer Agents from Natural Products*; Brahmachari, G., Ed.; Natural Product Drug Discovery; Elsevier, 2021; pp 283−294.

(24) Anajafi, T.; Mallik, S. Polymersome-Based Drug-Delivery Strategies for Cancer Therapeutics. *Ther. Delivery* **2015**, *6*, 521−534.

(25) Discher, D. E.; Ahmed, F. Polymersomes. *Annu. Rev. Biomed. Eng.* **2006**, *8*, 323−341.

(26) Discher, B. M.; Won, Y.-Y.; Ege, D. S.; Lee, J. C.-M.; Bates, F. S.; Discher, D. E.; Hammer, D. A. Polymersomes: Tough Vesicles Made from Diblock Copolymers. *Science* **1999**, *284*, 1143−1146.

(27) Nahire, R.; Haldar, M. K.; Paul, S.; Ambre, A. H.; Meghnani, V.; Layek, B.; Katti, K. S.; Gange, K. N.; Singh, J.; Sarkar, K.; Mallik, S. Multifunctional Polymersomes for Cytosolic Delivery of Gemcitabine and Doxorubicin to Cancer Cells. *Biomaterials* **2014**, *35*, 6482−6497.

(28) Karandish, F.; Mamnoon, B.; Feng, L.; Haldar, M. K.; Xia, L.; Gange, K. N.; You, S.; Choi, Y.; Sarkar, K.; Mallik, S. Nucleus-Targeted, Echogenic Polymersomes for Delivering a Cancer Stemness Inhibitor to Pancreatic Cancer Cells. *Biomacromolecules* **2018**, *19*, 4122−4132.

(29) Meng, F.; Zhong, Z.; Feijen, J. Stimuli-Responsive Polymersomes for Programmed Drug Delivery. *Biomacromolecules* **2009**, *10*, 197−209.

(30) Thambi, T.; Park, J. H.; Lee, D. S. Stimuli-Responsive Polymersomes for Cancer Therapy. *Biomater. Sci.* **2016**, *4*, 55−69.

(31) Liu, J.; Huang, Y.; Kumar, A.; Tan, A.; Jin, S.; Mozhi, A.; Liang, X.-J. PH-Sensitive Nano-Systems for Drug Delivery in Cancer Therapy. *Biotechnol. Adv.* **2014**, *32*, 693−710.

(32) McCarley, R. L. Redox-Responsive Delivery Systems. *Annu. Rev. Anal. Chem.* **2012**, *5*, 391−411.

(33) Ding, Y.; Kang, Y.; Zhang, X. Enzyme-Responsive Polymer Assemblies Constructed through Covalent Synthesis and Supramolecular Strategy. *Chem. Commun.* **2015**, *51*, 996−1003.

(34) Oliveira, H.; Pérez-Andrés, E.; Thevenot, J.; Sandre, O.; Berra, E.; Lecommandoux, S. Magnetic Field Triggered Drug Release from Polymersomes for Cancer Therapeutics. *J. Controlled Release* **2013**, *169*, 165−170.

(35) Egli, S.; Nussbaumer, M. G.; Balasubramanian, V.; Chami, M.; Bruns, N.; Palivan, C.; Meier, W. Biocompatible Functionalization of Polymersome Surfaces: A New Approach to Surface Immobilization and Cell Targeting Using Polymersomes. *J. Am. Chem. Soc.* **2011**, *133*, 4476−4483.

(36) Lale, S. V.; Kumar, A.; Prasad, S.; Bharti, A. C.; Koul, V. Folic Acid and Trastuzumab Functionalized Redox Responsive Polymersomes for Intracellular Doxorubicin Delivery in Breast Cancer. *Biomacromolecules* **2015**, *16*, 1736−1752.

(37) Zhong, Y.; Meng, F.; Deng, C.; Zhong, Z. Ligand-Directed Active Tumor-Targeting Polymeric Nanoparticles for Cancer Chemotherapy. *Biomacromolecules* **2014**, *15*, 1955−1969.

(38) Akhtar, M. J.; Ahamed, M.; Alhadlaq, H. A.; Alrokayan, S. A.; Kumar, S. Targeted Anticancer Therapy: Overexpressed Receptors and Nanotechnology. *Clin. Chim. Acta* **2014**, *436*, 78−92.

(39) Shreffler, J.; Koppelman, M.; Mamnoon, B.; Mallik, S.; Layek, B. 21 - Biopolymeric Systems for Diagnostic Applications. In *Tailor-Made and Functionalized Biopolymer Systems*; Bera, H.; Layek, B.; Singh, J., Eds.; Woodhead Publishing Series in Biomaterials; Woodhead Publishing, 2021; pp 705−722.

(40) Elledge, R. M.; Green, S.; Pugh, R.; Allred, D. C.; Clark, G. M.; Hill, J.; Ravdin, P.; Martino, S.; Osborne, C. K. Estrogen Receptor (ER) and Progesterone Receptor (PgR), by Ligand-Binding Assay Compared with ER, PgR and PS2, by Immuno-Histochemistry in Predicting Response to Tamoxifen in Metastatic Breast Cancer: A Southwest Oncology Group Study. *Int. J. Cancer* **2000**, *89*, 111−117.

(41) Zhang, Z.; Maier, B.; Santen, R. J.; Song, R. X.-D. Membrane Association of Estrogen Receptor α Mediates Estrogen Effect on MAPK Activation. *Biochem. Biophys. Res. Commun.* **2002**, *294*, 926−933.

(42) Yang, G.; Nowsheen, S.; Aziz, K.; Georgakilas, A. G. Toxicity and Adverse Effects of Tamoxifen and Other Anti-Estrogen Drugs. *Pharmacol. Ther.* **2013**, *139*, 392−404.

(43) Chang, M. Tamoxifen Resistance in Breast Cancer. *Biomol. Ther.* **2012**, *20*, 256−267.

(44) Jain, A. S.; Goel, P. N.; Shah, S. M.; Dhawan, V. V.; Nikam, Y.; Gude, R. P.; Nagarsenker, M. S. Tamoxifen Guided Liposomes for Targeting Encapsulated Anticancer Agent to Estrogen Receptor Positive Breast Cancer Cells: In Vitro and in Vivo Evaluation. *Biomed. Pharmacother.* **2014**, *68*, 429−438.

(45) Ahmad, A.; Ali, S. M.; Ahmad, M. U.; Sheikh, S.; Ahmad, I. Orally Administered Endoxifen Is a New Therapeutic Agent for Breast Cancer. *Breast Cancer Res. Treat.* **2010**, *122*, 579−584.

(46) Holmes, F. A.; Liticker, J. D. Pharmacogenomics of Tamoxifen in a Nutshell—And Who Broke the Nutcracker? *J. Oncol. Pract.* **2005**, *1*, 155−159.

(47) Agudelo, D.; Sanyakamdhorn, S.; Nafisi, S.; Tajmir-Riahi, H.-A. Transporting Antitumor Drug Tamoxifen and Its Metabolites, 4-Hydroxytamoxifen and Endoxifen by Chitosan Nanoparticles. *PLoS One* **2013**, *8*, No. e60250.

(48) Ding, S.; Qiao, X.; Kucera, G. L.; Bierbach, U. Design of a Platinum−Acridine−Endoxifen Conjugate Targeted at Hormone-Dependent Breast Cancer. *Chem. Commun.* **2013**, *49*, 2415−2417.

(49) Kelly, P. M.; Keely, N. O.; Bright, S. A.; Yassin, B.; Ana, G.; Fayne, D.; Zisterer, D. M.; Meegan, M. J. Novel Selective Estrogen Receptor Ligand Conjugates Incorporating Endoxifen-Combretastatin and Cyclofenil-Combretastatin Hybrid Scaffolds: Synthesis and Biochemical Evaluation. *Molecules* **2017**, *22*, No. 1440.

(50) Letchford, K.; Burt, H. A Review of the Formation and Classification of Amphiphilic Block Copolymer Nanoparticulate Structures: Micelles, Nanospheres, Nanocapsules and Polymersomes. *Eur. J. Pharm. Biopharm.* **2007**, *65*, 259−269.

(51) Patel, A.; Sant, S. Hypoxic Tumor Microenvironment: Opportunities to Develop Targeted Therapies. *Biotechnol. Adv.* **2016**, *34*, 803−812.

(52) Perche, F.; Biswas, S.; Wang, T.; Zhu, L.; Torchilin, V. P. Hypoxia-Targeted SiRNA Delivery. *Angew. Chem., Int. Ed.* **2014**, *53*, 3362−3366.

(53) Kiyose, K.; Hanaoka, K.; Oushiki, D.; Nakamura, T.; Kajimura, M.; Suematsu, M.; Nishimatsu, H.; Yamane, T.; Terai, T.; Hirata, Y.; Nagano, T. Hypoxia-Sensitive Fluorescent Probes for in Vivo Real-Time Fluorescence Imaging of Acute Ischemia. *J. Am. Chem. Soc.* **2010**, *132*, 15846−15848.

(54) Jung, H. J.; Min, H.; Yu, H.; Lee, T. G.; Chung, T. D. Electrochemical Cleavage of Azo Linkage for Site-Selective Immobilization and Cell Patterning. *Chem. Commun.* **2010**, *46*, 3863−3865.

(55) Jiang, J.; Auchinvole, C.; Fisher, K.; Campbell, C. J. Quantitative Measurement of Redox Potential in Hypoxic Cells Using SERS Nanosensors. *Nanoscale* **2014**, *6*, 12104−12110.

(56) Brownlee, W. J.; Seib, F. P. Impact of the Hypoxic Phenotype on the Uptake and Efflux of Nanoparticles by Human Breast Cancer Cells. *Sci. Rep.* **2018**, *8*, No. 12318.

(57) Neshatian, M.; Chung, S.; Yohan, D.; Yang, C.; Chithrani, D. B. Determining the Size Dependence of Colloidal Gold Nanoparticle Uptake in a Tumor-like Interface (Hypoxic). *Colloid Interface Sci. Commun.* **2014**, *1*, 57−61.

(58) Mencalha, A.; Victorino, V. J.; Cecchini, R.; Panis, C. Mapping Oxidative Changes in Breast Cancer: Understanding the Basic to Reach the Clinics. *Anticancer Res.* **2014**, *34*, 1127−1140.

(59) Stoner, M.; Saville, B.; Wormke, M.; Dean, D.; Burghardt, R.; Safe, S. Hypoxia Induces Proteasome-Dependent Degradation of Estrogen Receptor α in ZR-75 Breast Cancer Cells. *Mol. Endocrinol.* **2002**, *16*, 2231−2242.